Acta Crystallographica Section A
Foundations of Crystallography
ISSN 0108-7673

Received 4 January 1999
Accepted 2 July 1999

Minimal surfaces with self-intersections along straight lines. II. Surfaces forming three-periodic labyrinths

E. Koch

Institut für Mineralogie, Petrologie und Kristallographie der Universität Marburg, Hans-Meerwein-Strasse, D-35032 Marburg, Germany. Correspondence e-mail: kochelke@mailer.uni-marburg.de

47 families of minimal surfaces with straight self-intersections have been derived which subdivide R^3 into a finite number of congruent three-periodic labyrinths. In most of these cases, namely for 42 families, the number of labyrinths is two. Four congruent labyrinths have been found three times and eight congruent labyrinths twice. Minimal surfaces with three or six labyrinths seem not to exist. Most of these minimal surfaces are non-orientable. The surfaces of three families only are orientable ones.

1. Introduction

Each intersection-free three-periodic minimal surface is necessarily an orientable surface, *i.e.* it has two sides that may be coloured differently. As a consequence, it subdivides R^3 into two infinite three-periodic labyrinths that interpenetrate each other (*cf.* Fischer & Koch, 1996*b*; Koch & Fischer, 1999, and references cited therein). If there exists any straight line running within a minimal surface, this line is a twofold rotation axis and the surface is called a spanning minimal surface (Fischer & Koch, 1996*b*). The symmetry of a three-periodic spanning minimal surface without self-intersections is best described by a space-group pair *G*–*S*, where *G* means the full symmetry group of the non-oriented (uncoloured) surface and *S* stands for the symmetry of the oriented surface and, in addition, for the symmetry of each of the two labyrinths. *S* is always a subgroup of *G* with index 2.

In contrast to this, self-intersecting three-periodic minimal surfaces may be either orientable or non-orientable. They give rise to a variety of spatial subunits which may differ in their periodicity and connectivity (Fischer & Koch, 1996*b*). In the following, all those three-periodic minimal surfaces with straight self-intersections are treated that subdivide R^3 into three-periodic labyrinths and that could be derived by the methods described previously (Koch & Fischer, 1999). The generating polygons of all these surfaces have the following common property. There exist at least two polygon edges without a common vertex and without self-intersection of the surface along these edges. Except for the two families of minimal surfaces with eight labyrinths, these two edges do not run parallel to each other.

A new kind of reference symbol for three-periodic minimal surfaces with straight self-intersections will be used. The symbol of an orientable surface starts with OR, that of a non-orientable one with NO, followed by 3^2, 3^4 or 3^8, depending on the number $n_{\rm lab}$ of three-periodic labyrinths caused by the surface. Each symbol is completed by a small letter indicating the crystal system of the surface symmetry (c stands for cubic, h for hexagonal, t for tetragonal and o for orthorhombic) and an arbitrary numbering. Surfaces symbolized by oNO3^2–t1 are orthorhombic variants of tetragonal NO3^2–t1 surfaces.

2. Non-orientable minimal surfaces

Tables 1 and 2 describe the properties (*cf.* Koch & Fischer, 1999) of 44 families of non-orientable surfaces with straight self-intersections. In column 1, each family is designated by its reference symbol. Column 2 of Table 1 shows the full symmetry group *G* of the surface, completed by the site symmetry (if it is higher than 1) of the generating polygon. Column 3 describes the generating polygon itself. The Euler characteristic χ of the minimal surface, referred to a primitive unit cell of *G*, is given in column 4. The next column displays the number *b* of branch points per primitive unit cell of *G*. The number *l* of surface patches forming a shortest Moebius strip, *i.e.* a shortest odd-membered closed ring, is indicated in column 6. The next three columns refer to the labyrinths formed by the surface. The symmetry group $U_{\rm lab}$ of one labyrinth is described in column 7, the number $n_{\rm lab}$ of labyrinths is given in column 8, and the Euler characteristic $\chi_{\rm lab}$ of a labyrinth in column 9. It should be noticed that $\chi_{\rm lab}$ is always referred to a primitive unit cell of $U_{\rm lab}$, which may be *m* times larger than a primitive unit cell of *G*. To enable an easier comparison of χ and $\chi_{\rm lab}$, the last column of Table 1 shows the ratio $r = m\chi/\chi_{\rm lab}$.

For each minimal surface described in Table 1, the vertices of a generating polygon are listed in the second column of Table 2 in consecutive order. A single line separates the coordinate triplets of two vertices corresponding to a polygon edge without self-intersection. A double line indicates the intersection of two parts of the surface along the respective polygon edge, whereas the intersection of three, four or even six parts is symbolized by | 3 |, | 4 | or | 6 |, respectively. If a

vertex corresponds to a branch point of the surface, its coordinates are printed in bold type. Reference symbols used in previous papers (Fischer & Koch, 1996*a*,*b*) are shown in the last column of Table 2.

In contrast to orientable surfaces, the Euler characteristic χ of a non-orientable minimal surface may be an even or an odd number (*cf.* Table 1). The Euler characteristic χ_{lab} of a three-periodic labyrinth, however, is necessarily even, because χ_{lab} may also be interpreted as the Euler characteristic of the (necessarily orientable) surface of the labyrinth.

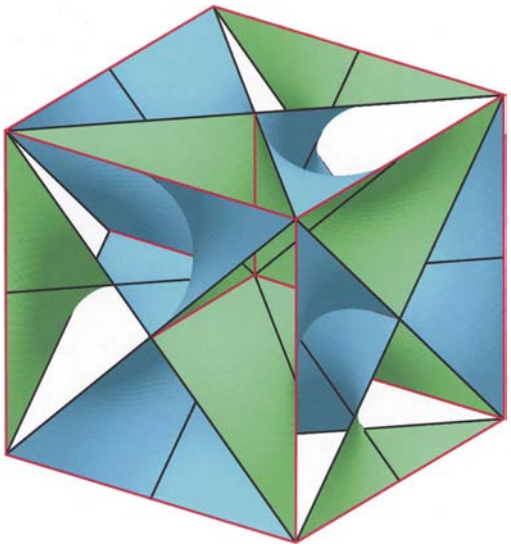

Figure 1
Part of an NO3^2–c2 surface with symmetry $G = I432$. One unit cell of $U_{lab} = P4_232$ is shown. Polygon edges with self-intersections are marked in red.

The following relation holds for all minimal surfaces giving rise to n_{lab} labyrinths:

$$r = m\chi/\chi_{lab} \geq \tfrac{1}{2}n_{lab}. \quad (1)$$

As a consequence, a labyrinth may be at most as complicated as the corresponding surface ($n_{lab} = 2$, $r = 1$). For 22 of the 39 families of non-orientable minimal surfaces with two labyrinths, r equals 1. This is true exactly for those surfaces that have exclusively lines of self-intersections that run parallel to each other or, at least, that do not intersect each other. In these cases only, each vertex of a generating polygon enters into the calculations of χ and χ_{lab} with the same weight [*cf.* Koch & Fischer (1999), formulae (3) and (7)]. The largest value $r = 5/2$ is observed for the NO3^2–c4 surfaces, a family already described by Schoen (1970).

The group–subgroup pair G–U_{lab} may be interpreted as a black–white space group in the case of $n_{lab} = 2$ or as a space group that permutes four or eight colours in the case of $n_{lab} = 4$ or $n_{lab} = 8$, respectively. For $n_{lab} = 2$, U_{lab} maps each labyrinth onto itself, whereas all symmetry operations from the coset of U_{lab} in G interchange the two (differently coloured) labyrinths. Figs. 1 to 4 show examples of self-intersecting non-orientable minimal surfaces forming two labyrinths. All pictures of minimal surfaces have been calculated with the aid of the program *SURFACE EVOLVER* (Brakke, 1992). The input files for *SURFACE EVOLVER* have been prepared by our own program *EVOLVERPREP*, which

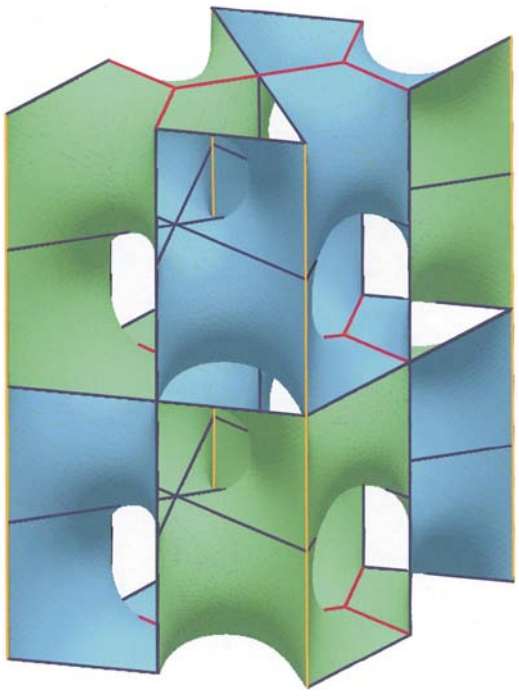

Figure 2
Part of an NO3^2–h8 surface with symmetry $P622$. One unit cell of $U_{lab} = P6_322$ (2**c**) is shown. Polygon edges with simple or threefold self-intersections are marked in red or in yellow, respectively. The common vertices of three red polygon edges are the branch points of the surface.

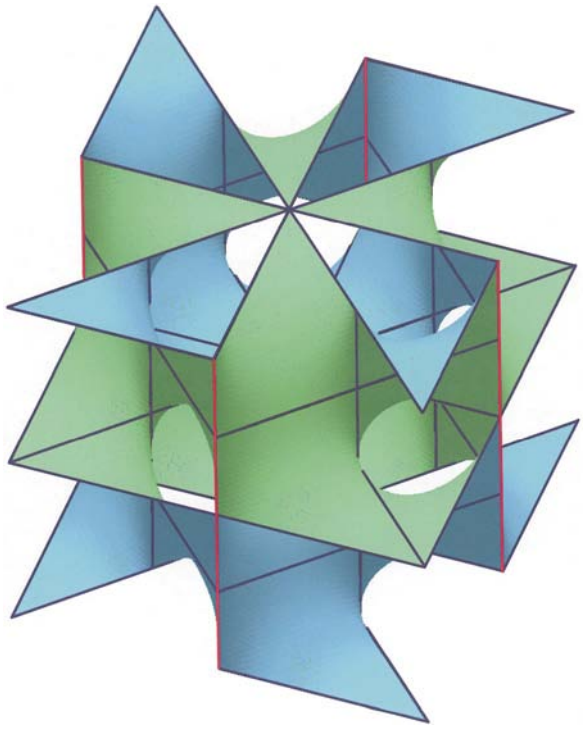

Figure 3
Part of an NO3^2–t4 surface with symmetry $G = P422$. One unit cell of $U_{lab} = I422$ (**a** − **b**, **a** + **b**, 2**c**) is shown. Polygon edges with self-intersection are marked in red.

generates the required copies of the original surface patch by means of the symmetry operations of the corresponding black–white or colour space group.

2.1. Minimal surfaces with four labyrinths

For $n_{lab} = 4$, the minimal value of r is 2. Three families of minimal surfaces with $n_{lab} = 4$ have been found, two with $r = 5/2$ ($NO3^4$–t1 and $NO3^4$–t2) and one with $r = 7/2$ ($NO3^4$–t3). In all three cases, G belongs to the space-group type $P422$ and U_{lab} is a class-equivalent subgroup of G (type $I4_122$) with index 4 and with $\mathbf{a}' = \mathbf{a} - \mathbf{b}$, $\mathbf{b}' = \mathbf{a} + \mathbf{b}$, $\mathbf{c}' = 4\mathbf{c}$. If referred to the generating polygons from Table 2, the labyrinths may be represented by the same labyrinth graphs in all three cases: Considered together, the vertices of all four labyrinth graphs of such a surface form a point configuration of $P422$ 4(i) $0, \frac{1}{2}, z$ with $z = \frac{1}{4}$ (*cf.* Fig. 5). The vertex at $0, \frac{1}{2}, \frac{1}{4}$ is connected to those at $1, \frac{1}{2}, -\frac{1}{4}$, at $-1, \frac{1}{2}, -\frac{1}{4}$, at $\frac{1}{2}, 1, -\frac{1}{4}$ and at $-\frac{1}{2}, 0, -\frac{1}{4}$.

Fig. 6 shows the relations between the groups G, U_{lab}, $N_E(G)$, $N_E(U_{lab})$ and $G \cap N_E(U_{lab})$, where $N_E(G)$ and $N_E(U_{lab})$ are the Euclidean normalizers of G and U_{lab}, respectively (*cf. International Tables for Crystallography*, 1987, Vol. A, ch. 15). The index 4 of U_{lab} in G corresponds to the four congruent labyrinths of each surface. As the index of $G \cap N_E(U_{lab})$ in G equals 2, each space group of type $P422$ has two conjugate subgroups of type $I4_122$ with $\mathbf{a}' = \mathbf{a} - \mathbf{b}$, $\mathbf{b}' = \mathbf{a} + \mathbf{b}$, $\mathbf{c}' = 4\mathbf{c}$. They are shifted against each other by the vector $\mathbf{c}$. The first of these subgroups maps, for example, each of the labyrinths 1 and 3 onto itself, but interchanges the labyrinths 2 and 4. Then, the second subgroup $I4_122$ maps each of the labyrinths 2 and 4 onto itself and interchanges 1 and 3. Two labyrinths with the same labyrinth group are shifted against each other by the vector $2\mathbf{c}$. Any of the four labyrinths is adjacent to the other two labyrinths that have a different labyrinth group, *i.e.* labyrinth 1 is adjacent to labyrinths 2 and 4, but is not adjacent to 3, and so on.

As the index of G in $N_E(G)$ is 8, for each of the families $NO3^4$–t1, $NO3^4$–t2, and $NO3^4$–t3 there exist eight congruent minimal surfaces with identical symmetry group $P422$. According to the index 16 of $G \cap N_E(U_{lab})$ in $N_E(G)$, the total number of Euclidean-equivalent subgroups of type $I4_122$ with $\mathbf{a}' = \mathbf{a} - \mathbf{b}$, $\mathbf{b}' = \mathbf{a} + \mathbf{b}$, $\mathbf{c}' = 4\mathbf{c}$ is 16. They may be grouped into eight pairs of conjugate subgroups, each of them referring to another minimal surface out of each family.

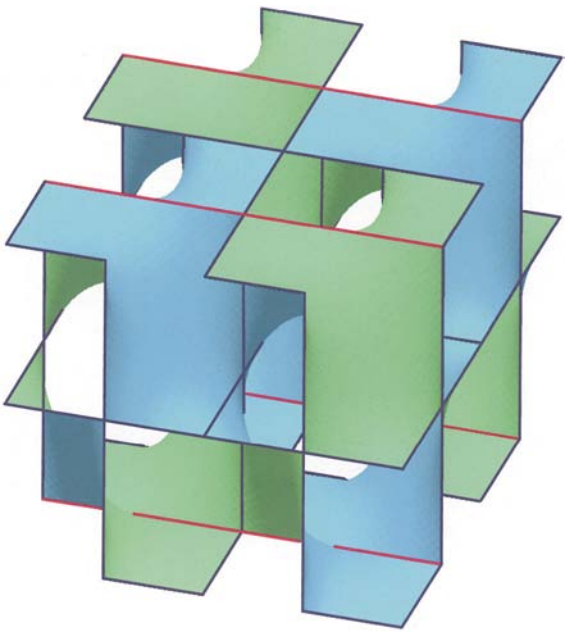

Figure 4
Part of an $NO3^2$–o4 surface with symmetry $G = P222$. One unit cell of $U_{lab} = C222$ ($2\mathbf{a}$, $2\mathbf{b}$) is shown. Polygon edges with self-intersections are marked in red.

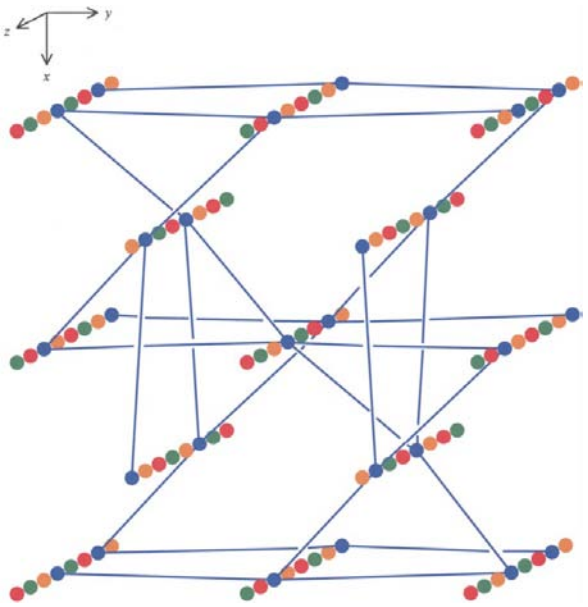

Figure 5
Vertices of the four labyrinth graphs of an $NO3^4$–t1, an $NO3^4$–t2 or an $NO3^4$–t3 surface. Edges are shown only for one labyrinth graph.

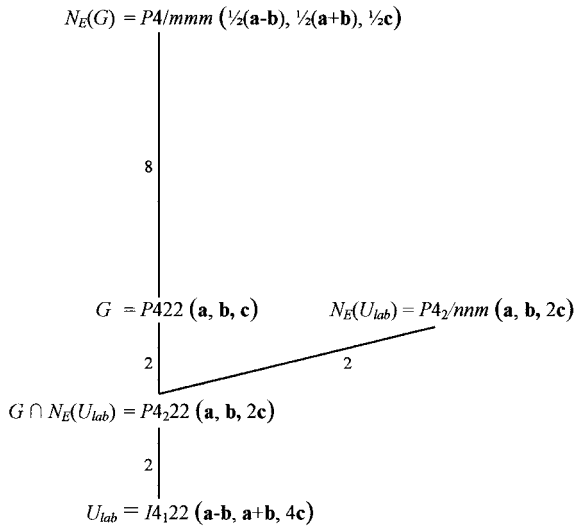

Figure 6
Subgroup diagram referring to an $NO3^4$–t1, $NO3^4$–t2 or $NO3^4$–t3 surface (G: symmetry group of the minimal surface; $N_E(G)$: Euclidean normalizer of G; U_{lab}: symmetry group of a labyrinth; $N_E(U_{lab})$: Euclidean normalizer of U_{lab}; $G \cap N_E(U)$: intersection group of G and $N_E(U_{lab})$.

Table 1
Non-orientable minimal surfaces.

Minimal surface						Labyrinths			
Symbol	Symmetry group G	Generating polygon	χ	b	l	Symmetry group U_{lab}	n_{lab}	χ_{lab}	$r = m\chi/\chi_{lab}$
$NO3^2$–c1	$Pn\bar{3}m$–..m	6-gon	−14	–	5	$Fd\bar{3}m$ (2**a**, 2**b**, 2**c**)	2	−24	7/6
$NO3^2$–c2	$I432$–..2	4-gon	−3	–	11	$P4_232$	2	−4	3/2
$NO3^2$–c3	$I432$	6-gon	−20	–	5	$I23$	2	−16	5/4
$NO3^2$–c4	$I4_132$	5-gon	−10	4	7	$P4_132$	2	−8	5/2
$NO3^2$–h1	$P6/mcc$–m..	8-gon	−14	4	5	$P\bar{6}c2$	2	−8	7/4
$NO3^2$–h2	$P6/mcc$–m..	8-gon	−14	–	7	$P6/m$	2	−14	1
$NO3^2$–h3	$P6/mcc$–m..	8-gon	−18	–	5	$P6/m$	2	−18	1
$NO3^2$–h4	$P622$–..2	8-gon	−7	–	7	$P622$ (2**c**)	2	−14	1
$NO3^2$–h5	$P622$–..2	8-gon	−9	–	5	$P622$ (2**c**)	2	−18	1
$NO3^2$–h6	$P622$	6-gon	−7	2	5	$P312$	2	−4	7/4
$NO3^2$–h7	$P622$	7-gon	−11	2	5	$P6_322$ (2**c**)	2	−16	11/8
$NO3^2$–h8	$P622$	7-gon	−11	2	5	$P6_322$ (2**c**)	2	−16	11/8
$NO3^2$–h9	$P622$	7-gon	−13	2	5	$P6_322$ (2**c**)	2	−16	13/8
$NO3^2$–h10	$P6_222$–..2	6-gon	−3	–	7	$P6_422$ (2**c**)	2	−6	1
$NO3^2$–t1	$P4/mcc$–m..	6-gon	−6	–	7	$P4/mnc$ (**a** − **b**, **a** + **b**)	2	−12	1
$NO3^2$–t2	$P4/mcc$–m..	8-gon	−10	–	5	$P4/m$	2	−10	1
$NO3^2$–t3	$P422$–.2.	8-gon	−5	–	5	$P422$ (2**c**)	2	−10	1
$NO3^2$–t4	$P422$	5-gon	−3	–	7	$I422$ (**a** − **b**, **a** + **b**, 2**c**)	2	−6	1
$NO3^2$–t5	$P422$	6-gon	−4	–	9	$I422$ (**a** − **b**, **a** + **b**, 2**c**)	2	−8	1
$NO3^2$–t6	$P422$	7-gon	−7	–	5	$I422$ (**a** − **b**, **a** + **b**, 2**c**)	2	−12	7/6
$NO3^2$–t7	$P422$	7-gon	−7	–	7	$I422$ (**a** − **b**, **a** + **b**, 2**c**)	2	−12	7/6
$NO3^2$–t8	$P422$	7-gon	−8	–	5	$I422$ (**a** − **b**, **a** + **b**, 2**c**)	2	−12	4/3
$NO3^2$–t9	$P422$	8-gon	−9	–	3	$I422$ (**a** − **b**, **a** + **b**, 2**c**)	2	−16	9/8
$NO3^2$–t10	$P4_222$	6-gon	−4	–	5	$I4_122$ (**a** − **b**, **a** + **b**, 2**c**)	2	−8	1
$NO3^2$–t11	$P4_222$	6-gon	−4	–	9	$I4_122$ (**a** − **b**, **a** + **b**, 2**c**)	2	−8	1
$NO3^2$–t12	$P4_222$	7-gon	−6	–	5	$I4_122$ (**a** − **b**, **a** + **b**, 2**c**)	2	−8	3/2
$NO3^2$–t13	$P4_222$	8-gon	−8	–	5	$I4_122$ (**a** − **b**, **a** + **b**, 2**c**)	2	−16	1
$NO3^2$–t14	$P4_222$	8-gon	−8	–	5	$P4_22_12$ (**a** − **b**, **a** + **b**)	2	−16	1
$NO3^2$–t15	$P4_222$	8-gon	−8	–	3	$P4_2$	2	−8	1
$NO3^2$–t16	$P4_222$	8-gon	−8	–	3	$P4_322$ (2**c**)	2	−16	1
$NO3^2$–t17	$P4_222$	9-gon	−10	–	3	$P4_322$ (2**c**)	2	−16	5/4
$NO3^2$–o1	$Pccm$–..m	8-gon	−4	–	5	$Cccm$ (2**a**, 2**b**)	2	−8	1
$NO3^2$–o2	$Pccm$–..m	10-gon	−6	–	3	$P112/m$	2	−6	1
$NO3^2$–o3	$P222$–2..	10-gon	−3	–	3	$P222$ (2**c**)	2	−6	1
$NO3^2$–o4	$P222$	7-gon	−3	–	5	$C222$ (2**a**, 2**b**)	2	−6	1
$NO3^2$–o5	$P222$	9-gon	−5	–	3	$C222$ (2**a**, 2**b**)	2	−8	5/4
$NO3^2$–o6	$P222$	9-gon	−5	–	3	$C222$ (2**a**, 2**b**)	2	−10	1
o$NO3^2$–t5	$P222$	7-gon	−3	–	5	$F222$ (2**a**, 2**b**, 2**c**)	2	−6	1
$NO3^2$–o7	$P222$	11-gon	−7	–	3	$F222$ (2**a**, 2**b**, 2**c**)	2	−12	7/6
$NO3^4$–t1	$P422$	6-gon	−5	–	7	$I4_122$ (**a** − **b**, **a** + **b**, 4**c**)	4	−8	5/2
$NO3^4$–t2	$P422$	6-gon	−5	–	7	$I4_122$ (**a** − **b**, **a** + **b**, 4**c**)	4	−8	5/2
$NO3^4$–t3	$P422$	7-gon	−7	–	5	$I4_122$ (**a** − **b**, **a** + **b**, 4**c**)	4	−8	7/2
$NO3^8$–t1	$P4_2/nbc$–$\bar{1}$	8-gon	−8	–	5	$I\bar{4}2d$ (2**a**, 2**b**, 2**c**)	8	−4	4
$NO3^8$–t2	$I422$–..2	6-gon	−3	–	7	$I4_122$ (2**a**, 2**b**, 2**c**)	8	−4	6

The four-colour space group corresponding to one of the pairs $P422$–$I4_122$ (**a** − **b**, **a** + **b**, 4**c**) may be generated by the same generators as $P422$ (*cf. International Tables for Crystallography*, 1987, Vol. A), each supplemented by a permutation of four elements, *e.g.* by

$$
\begin{aligned}
&t \quad (1,0,0) \quad (13)(24),\\
&t \quad (0,1,0) \quad (13)(24),\\
&t \quad (0,0,1) \quad (1432),\\
&2 \quad 0,0,z \quad (13)(24),\\
&4^+ \quad 0,0,z \quad (1432),\\
&2 \quad 0,y,0 \quad (1)(3)(24).
\end{aligned}
$$

The respective group of permutations of four elements (or four colours) has order 8 and is isomorphic to a crystallographic point group of type 422. As already shown by the generators, it contains even as well as odd permutations. It is the p-Sylow group ($p = 2$) in S_4, where S_4 is the symmetric group of degree 4, *i.e.* the group of all permutations of four elements (*cf. e.g.* Hall & Senior, 1964). Fig. 7 shows part of an $NO3^4$–t1 surface with the four labyrinths coloured differently.

2.2. Minimal surfaces with eight labyrinths

For $n_{lab} = 8$, the minimal value of r equals 4. Two families of minimal surfaces with eight labyrinths have been found so far, namely $NO3^8$–t1 with $r = 4$ and $NO3^8$–t2 with $r = 6$. Although

Table 2
Generating polygons of non-orientable minimal surfaces.

Symbol	Generating polygon	Previous symbol
NO3^2–c1	$000 \parallel \frac{1}{2}00 \mid \frac{1}{2}\frac{1}{4}0 \mid \frac{1}{4}\frac{1}{4}\frac{1}{4} \mid \frac{1}{4}\frac{1}{2}0 \mid 0\frac{1}{2}0 \parallel$	
NO3^2–c2	$000 \mid \frac{1}{2}\frac{1}{2}0 \parallel \frac{1}{2}\frac{1}{2}\frac{1}{2} \mid 0\frac{1}{2}0 \parallel$	WF–3^2
NO3^2–c3	$000 \parallel \frac{1}{2}00 \parallel \frac{1}{2}\frac{1}{4}0 \mid \frac{1}{4}\frac{1}{4}\frac{1}{4} \mid \frac{1}{4}\frac{1}{2}0 \parallel \frac{1}{2}\frac{1}{2}0 \mid$	
NO3^2–c4	$\frac{1}{8}\frac{1}{8}\frac{1}{8} \mid \frac{11}{48}0 \mid \frac{1}{4}\frac{5}{8}0 \parallel \mathbf{\frac{15}{88}\ \frac{-1}{8}} \parallel \frac{1}{8}\frac{1}{2}\ {-\frac{1}{4}} \mid$	CBP1–3^2
NO3^2–h1	$00\frac{1}{4} \mid \frac{1}{2}0\frac{1}{4} \parallel \mathbf{2/3\ 1/3}\ \frac{1}{4} \parallel \frac{1}{2}\frac{1}{2}\frac{1}{4} \mid \frac{1}{2}\frac{1}{2}\frac{3}{4} \parallel \mathbf{2/3\ 1/3}\ \frac{3}{4} \parallel \frac{1}{2}0\frac{3}{4} \mid 00\frac{3}{4} \mid 3 \mid$	HBP1–3^2
NO3^2–h2	$00\frac{1}{4} \mid \frac{1}{2}0\frac{1}{4} \mid 2/3\ 1/3\ \frac{1}{4} \mid 10\frac{1}{4} \mid 6 \mid 10\frac{3}{4} \mid 2/3\ 1/3\ \frac{3}{4} \mid \frac{1}{2}0\frac{3}{4} \mid 00\frac{3}{4} \mid 6 \mid$	
NO3^2–h3	$00\frac{1}{4} \mid \frac{1}{2}0\frac{1}{4} \parallel \frac{1}{2}0\frac{3}{4} \mid 00\frac{3}{4} \mid 2/3\ 1/3\ \frac{3}{4} \mid \frac{1}{2}\frac{1}{2}\frac{3}{4} \parallel \frac{1}{2}\frac{1}{2}\frac{1}{4} \mid 2/3\ 1/3\ \frac{1}{4} \mid$	
NO3^2–h4	$000 \mid 2/3\ 1/3\ 0 \mid \frac{1}{2}\frac{1}{2}0 \mid 110 \mid 6 \mid 111 \mid 2/3\ 1/3\ 1 \mid \frac{1}{2}\frac{1}{2}1 \mid 001 \mid 6 \mid$	HAS1–3^2
NO3^2–h5	$000 \mid 2/3\ 1/3\ 0 \mid \frac{1}{2}00 \parallel \frac{1}{2}01 \mid 001 \mid 2/3\ 1/3\ 1 \mid \frac{1}{2}\frac{1}{2}1 \parallel \frac{1}{2}\frac{1}{2}0 \mid$	ALB–3^2
NO3^2–h6	$000 \mid \frac{1}{2}00 \parallel \mathbf{2/3\ 1/3\ 0} \parallel \frac{1}{2}\frac{1}{2}0 \mid \frac{1}{2}\frac{1}{2}\frac{1}{2} \mid 00\frac{1}{2} \mid 3 \mid$	HBP2–3^2
NO3^2–h7	$000 \mid \frac{1}{2}00 \parallel \mathbf{2/3\ 1/3\ 0} \parallel \frac{1}{2}\frac{1}{2}0 \mid \frac{1}{2}\frac{1}{2}\frac{1}{2} \mid 1/3\ 2/3\ \frac{1}{2} \mid 00\frac{1}{2} \mid 3 \mid$	HBP3–3^2
NO3^2–h8	$000 \mid \frac{1}{2}00 \parallel \mathbf{2/3\ 1/3\ 0} \parallel \frac{1}{2}\frac{1}{2}0 \mid \frac{1}{2}\frac{1}{2}\frac{1}{2} \mid 2/3\ 1/3\ \frac{1}{2} \mid 00\frac{1}{2} \mid 3 \mid$	HBP4–3^2
NO3^2–h9	$000 \parallel \mathbf{2/3\ 1/3\ 0} \parallel 100 \mid \frac{1}{2}00 \mid \frac{1}{2}0\frac{1}{2} \mid 2/3\ 1/3\ \frac{1}{2} \mid 00\frac{1}{2} \mid 3 \mid$	
NO3^2–h10	$000 \mid \frac{1}{2}00 \mid 110 \parallel 11\ {-1/3} \mid 1\frac{1}{2}\ {-1/3} \mid 00\ {-1/3} \parallel$	Q–3^2
NO3^2–t1	$00\frac{1}{4} \mid \frac{1}{2}0\frac{1}{4} \mid \frac{1}{2}0\frac{3}{4} \mid 00\frac{3}{4} \mid \frac{1}{2}\frac{1}{2}\frac{3}{4} \parallel \frac{1}{2}\frac{1}{2}\frac{1}{4} \mid$	TAD1–3^2
NO3^2–t2	$00\frac{1}{4} \mid \frac{1}{2}0\frac{1}{4} \mid \frac{1}{2}\frac{1}{2}\frac{1}{4} \mid 10\frac{1}{4} \mid 4 \mid 10\frac{3}{4} \mid \frac{1}{2}\frac{1}{2}\frac{3}{4} \mid \frac{1}{2}0\frac{3}{4} \mid 00\frac{3}{4} \mid 4 \mid$	
NO3^2–t3	$000 \mid \frac{1}{2}\frac{1}{2}0 \mid \frac{1}{2}00 \mid 100 \mid 4 \mid 101 \mid \frac{1}{2}\frac{1}{2}1 \mid \frac{1}{2}01 \mid 001 \mid 4 \mid$	
NO3^2–t4	$000 \mid \frac{1}{2}00 \mid \frac{1}{2}0\frac{1}{2} \mid \frac{1}{2}\frac{1}{2}\frac{1}{2} \parallel \frac{1}{2}\frac{1}{2}0 \mid$	TAD2–3^2
NO3^2–t5	$000 \mid \frac{1}{2}\frac{1}{2}0 \parallel \frac{1}{2}\frac{1}{2}\frac{1}{2} \mid \frac{1}{2}0\frac{1}{2} \mid \frac{1}{2}01 \mid 001 \mid 4 \mid$	
NO3^2–t6	$000 \parallel \frac{1}{2}00 \mid \frac{1}{2}0\frac{1}{2} \mid 00\frac{1}{2} \mid \frac{1}{2}\frac{1}{2}\frac{1}{2} \parallel \frac{1}{2}\frac{1}{2}0 \mid 0\frac{1}{2}0 \parallel$	
NO3^2–t7	$000 \parallel \frac{1}{2}00 \mid \frac{1}{2}0\frac{1}{2} \mid 10\frac{1}{2} \mid \frac{1}{2}\frac{1}{2}\frac{1}{2} \parallel \frac{1}{2}\frac{1}{2}0 \mid 0\frac{1}{2}0 \parallel$	
NO3^2–t8	$000 \parallel \frac{1}{2}\frac{1}{2}0 \parallel 100 \mid \frac{1}{2}00 \mid \frac{1}{2}0\frac{1}{2} \mid \frac{1}{2}\frac{1}{2}\frac{1}{2} \mid 00\frac{1}{2} \parallel$	
NO3^2–t9	$000 \mid \frac{1}{2}\frac{1}{2}0 \parallel \frac{1}{2}00 \mid \frac{1}{2}0\frac{1}{2} \mid \frac{1}{2}\frac{1}{2}\frac{1}{2} \parallel \frac{1}{2}\frac{1}{2}1 \parallel \frac{1}{2}01 \mid 001 \mid 4 \mid$	
NO3^2–t10	$000 \mid \frac{1}{2}00 \mid \frac{1}{2}\frac{1}{2}0 \mid \frac{1}{2}\frac{1}{2}\frac{1}{4} \mid 01\frac{1}{4} \mid 010 \parallel$	
NO3^2–t11	$000 \mid \frac{1}{2}00 \parallel \frac{1}{2}01 \mid \frac{1}{2}\frac{1}{2}1 \mid \frac{1}{2}\frac{1}{2}\frac{3}{4} \mid 00\frac{3}{4} \mid 3 \mid$	
NO3^2–t12	$000 \parallel 100 \mid 3 \mid 10\frac{1}{4} \mid \frac{1}{2}\frac{1}{2}\frac{1}{4} \mid \frac{1}{2}\frac{1}{2}\frac{1}{2} \mid \frac{1}{2}0\frac{1}{2} \mid 00\frac{1}{2} \mid 3 \mid$	
NO3^2–t13	$000 \mid \frac{1}{2}00 \mid \frac{1}{2}\ {-\frac{1}{2}}0 \mid \frac{1}{2}\ {-\frac{1}{2}}\frac{1}{4} \parallel 00\frac{1}{4} \mid \frac{1}{2}\frac{1}{2}\frac{1}{4} \parallel 01\frac{1}{4} \mid 010 \parallel$	
NO3^2–t14	$000 \mid \frac{1}{2}00 \mid \frac{1}{2}0\frac{1}{2} \mid 00\frac{1}{2} \parallel 00\frac{3}{4} \mid \frac{1}{2}\frac{1}{2}\frac{3}{4} \parallel \frac{1}{2}\frac{1}{2}\frac{1}{4} \parallel 00\frac{1}{4} \parallel$	
NO3^2–t15	$000 \mid 0\frac{1}{2}0 \mid \frac{1}{2}\frac{1}{2}0 \mid \frac{1}{2}10 \mid 010 \parallel 01\frac{1}{4} \mid \frac{1}{2}\frac{1}{2}\frac{1}{4} \mid 00\frac{1}{4} \parallel$	
NO3^2–t16	$000 \parallel \frac{1}{2}00 \mid \frac{1}{2}\frac{1}{2}0 \mid \frac{1}{2}\frac{1}{2}\frac{1}{4} \mid 00\frac{1}{4} \mid 00\frac{1}{2} \parallel 0\frac{1}{2}\frac{1}{2} \mid 0\frac{1}{2}0 \mid$	TS1–3^2
NO3^2–t17	$000 \parallel \frac{1}{2}00 \mid \frac{1}{2}\frac{1}{2}0 \mid 3 \mid \frac{1}{2}\frac{1}{2}\frac{3}{4} \mid 00\frac{3}{4} \mid 3 \mid 001 \parallel \frac{1}{2}01 \mid \frac{1}{2}0\frac{1}{2} \mid 00\frac{1}{2} \mid 3 \mid$	
NO3^2–o1	$00\frac{1}{4} \mid \frac{1}{2}0\frac{1}{4} \parallel \frac{1}{2}1\frac{1}{4} \mid \frac{1}{2}1\frac{3}{4} \parallel \frac{1}{2}0\frac{3}{4} \mid 00\frac{3}{4} \mid 0\frac{1}{2}\frac{3}{4} \mid 0\frac{1}{2}\frac{1}{4} \mid$	
NO3^2–o2	$00\frac{1}{4} \mid \frac{1}{2}0\frac{1}{4} \parallel \frac{1}{2}0\frac{3}{4} \mid 00\frac{3}{4} \mid 0\frac{1}{2}\frac{3}{4} \mid \frac{1}{2}\frac{1}{2}\frac{3}{4} \mid \frac{1}{2}1\frac{3}{4} \parallel \frac{1}{2}1\frac{1}{4} \mid \frac{1}{2}\frac{1}{2}\frac{1}{4} \mid 0\frac{1}{2}\frac{1}{4} \mid$	
NO3^2–o3	$000 \mid \frac{1}{2}00 \parallel \frac{1}{2}01 \mid \frac{1}{2}\frac{1}{2}1 \mid 0\frac{1}{2}1 \mid 011 \mid \frac{1}{2}11 \parallel \frac{1}{2}10 \mid \frac{1}{2}\frac{1}{2}0 \mid 0\frac{1}{2}0 \mid$	
NO3^2–o4	$000 \mid \frac{1}{2}00 \parallel \frac{1}{2}10 \mid \frac{1}{2}1\frac{1}{2} \mid 01\frac{1}{2} \mid 0\frac{1}{2}\frac{1}{2} \mid 0\frac{1}{2}0 \mid$	
NO3^2–o5	$000 \parallel 0\frac{1}{2}0 \parallel 0\frac{1}{2}1 \parallel 001 \mid \frac{1}{2}01 \mid \frac{1}{2}\frac{1}{2}1 \mid \frac{1}{2}\frac{1}{2}\frac{1}{2} \mid \frac{1}{2}0\frac{1}{2} \mid 00\frac{1}{2} \mid$	
NO3^2–o6	$000 \mid 00\frac{1}{2} \mid \frac{1}{2}0\frac{1}{2} \parallel \frac{1}{2}00 \mid \frac{1}{2}\frac{1}{2}0 \mid \frac{1}{2}\frac{1}{2}\frac{1}{2} \mid \frac{1}{2}1\frac{1}{2} \parallel \frac{1}{2}10 \mid 010 \parallel$	
oNO3^2–t5	$000 \mid \frac{1}{2}00 \mid \frac{1}{2}\frac{1}{2}0 \mid \frac{1}{2}\frac{1}{2}\frac{1}{2} \mid 0\frac{1}{2}\frac{1}{2} \mid 01\frac{1}{2} \mid 010 \parallel$	oTAD2–3^2
NO3^2–o7	$000 \parallel \frac{1}{2}00 \mid \frac{1}{2}0\frac{1}{2} \parallel \frac{1}{2}1\frac{1}{2} \mid 01\frac{1}{2} \parallel 010 \parallel \frac{1}{2}10 \mid \frac{1}{2}\frac{1}{2}0 \mid 0\frac{1}{2}0 \mid 0\frac{1}{2}\frac{1}{2} \mid 00\frac{1}{2} \parallel$	
NO3^4–t1	$000 \parallel 00\frac{1}{2} \mid 0\frac{1}{2}\frac{1}{2} \mid \frac{1}{2}\frac{1}{2}\frac{1}{2} \parallel \frac{1}{2}\frac{1}{2}0 \mid 010 \parallel$	TS2–3^4
NO3^4–t2	$000 \parallel 00\frac{1}{2} \parallel 0\frac{1}{2}\frac{1}{2} \mid \frac{1}{2}\frac{1}{2}\frac{1}{2} \parallel \frac{1}{2}\frac{1}{2}0 \mid 100 \mid$	TS3–3^4
NO3^4–t3	$000 \parallel 010 \parallel 01\frac{1}{2} \mid 3 \mid 00\frac{1}{2} \mid 3 \mid \frac{1}{2}0\frac{1}{2} \mid \frac{1}{2}\frac{1}{2}\frac{1}{2} \parallel \frac{1}{2}\frac{1}{2}0 \mid$	
NO3^8–t1	$0\ {-\frac{1}{2}}0 \mid \frac{1}{2}00 \parallel \frac{1}{2}0\frac{1}{4} \parallel \frac{1}{2}1\frac{1}{4} \parallel \frac{1}{2}1\frac{1}{2} \mid 0\frac{1}{2}\frac{1}{2} \parallel 0\frac{1}{2}\frac{1}{4} \parallel 0\ {-\frac{1}{2}}\frac{1}{4} \parallel$	
NO3^8–t2	$000 \parallel 00\frac{1}{2} \parallel 10\frac{1}{2} \mid \frac{1}{2}\frac{1}{2}\frac{1}{2} \parallel \frac{1}{2}\frac{1}{2}0 \parallel \frac{1}{2}\ {-\frac{1}{2}}0 \mid$	TS4–3^8

they differ in their symmetry (*cf.* Table 1), they have several properties in common.

The symmetry group G of an NO3^8–t1 surface belongs to type $P4_2/nbc$, the symmetry group $U_{\rm lab}$ of each of its labyrinths to type $I\bar{4}2d$ with $\mathbf{a}' = 2\mathbf{a}$, $\mathbf{b}' = 2\mathbf{b}$ and $\mathbf{c}' = 2\mathbf{c}$. The index 8 of $U_{\rm lab}$ in G (*cf.* Fig. 8) equals the number of congruent labyrinths of such a surface. As the index of $G \cap N_E(U_{\rm lab})$ in $N_E(G)$ is 16, each space group of type $P4_2/nbc$ has 16 Euclidean-equivalent subgroups of type $I\bar{4}2d$ with $\mathbf{a}' = 2\mathbf{a}$, $\mathbf{b}' = 2\mathbf{b}$, $\mathbf{c}' = 2\mathbf{c}$. According to the index 4 of $G \cap N_E(U_{\rm lab})$ in G, four times four of these subgroups are conjugate in G. As a consequence, the eight labyrinths of an NO3^8–t1 surface correspond to four conjugate labyrinth groups, *i.e.* four times two of these labyrinths have identical labyrinth symmetry and are shifted against each other by a vector $\mathbf{c}$.

Given a first labyrinth group of an NO3^8–t1 surface, a second one may be derived with the aid of a translation by a vector $\mathbf{a}$. Then, all 2.., 2_1.., .2. and .2_1. axes and the positions of

the ..*d* glide-reflection planes coincide for both groups, whereas the *z* coordinates of their $\bar{4}$ roto-inversion centres and the directions of their glide vectors differ. Inversion through the symmetry centre, *e.g.* at $\frac{1}{4}, \frac{1}{4}, \frac{1}{4}$ (referred to origin choice 1 of $P4_2/nbc$), yields the other two labyrinth groups. Their $\bar{4}$ and 2_1.. axes have interchanged positions in comparison with the first two labyrinth groups.

Any one of the eight labyrinths of an NO3^8–t1 surface is adjacent to four other labyrinths belonging to two different labyrinth groups. The 2_1.. axes of the original labyrinth coincide with the $\bar{4}$ axes of the four neighbouring labyrinths.

Considered together, the vertices of the eight labyrinth graphs corresponding to an NO3^8–t1 surface as described in Table 2 form a point configuration 4(*d*) 0, 0, 0 of $P4_2/nbc$, *i.e.* a tetragonal C_c configuration (*cf. International Tables for Crystallography*, 1987, Vol. A, ch. 14). The vertex at 0, 0, 0 is connected to four other vertices, namely to 0, 1, $\frac{1}{2}$, to 0, -1, $\frac{1}{2}$, to 1, 0, $-\frac{1}{2}$ and to -1, 0, $-\frac{1}{2}$ (*cf.* Fig. 9). The vertices of a single labyrinth graph correspond to a tetragonal deformed *D* configuration.

According to the index 4 of *G* in $N_E(G)$, there exist four congruent NO3^8–t1 surfaces with identical symmetry group *G* but with different labyrinth groups $U_{\rm lab}$.

The eight-colour space group corresponding to a certain group–subgroup pair $P4_2/nbc$–$I\bar{4}2d$ (2**a**, 2**b**, 2**c**) may be generated for example by the following pairs of symmetry operations and permutations of eight elements or colours:

t (1, 0, 0) (14)(23)(58)(67),
t (0, 1, 0) (13)(24)(57)(68),
t (0, 0, 1) (12)(34)(56)(78),
2 0, 0, z (1)(2)(3)(4)(56)(78),
4^+ (0, 0, $\frac{1}{2}$) 0, $\frac{1}{2}$, z (1835)(2746),
2 0, y, $\frac{1}{4}$ (14)(23)(58)(67),
$\bar{1}$ $\frac{1}{4}, \frac{1}{4}, \frac{1}{4}$ (18)(27)(36)(45).

The generated permutation group has the order 64 and consists of even permutations only. It is not isomorphic to

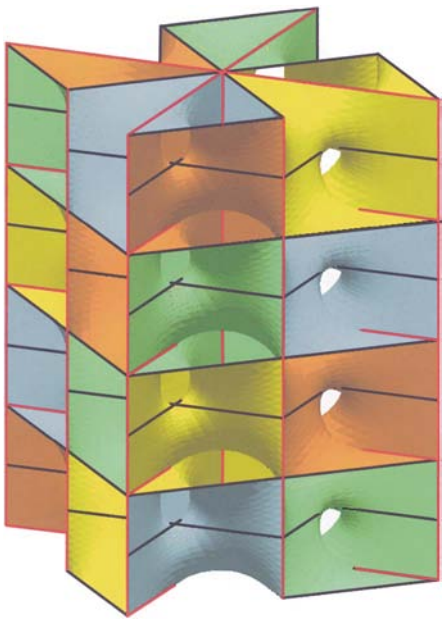

Figure 7
Part of an NO3^4–t1 surface with symmetry $G = P422$. One unit cell of $U_{\rm lab} = I4_122$ (**a** − **b**, **a** + **b**, 4**c**) is shown. Polygon edges with self-intersections are marked in red.

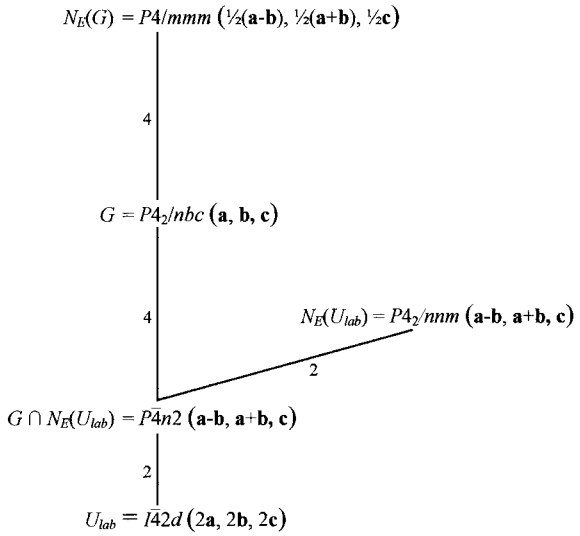

Figure 8
Subgroup diagram referring to an NO3^8–t1 surface [*G*: symmetry group of the minimal surface; $N_E(G)$: Euclidean normalizer of *G*; $U_{\rm lab}$: symmetry group of a labyrinth; $N_E(U_{\rm lab})$: Euclidean normalizer of $U_{\rm lab}$; $G \cap N_E(U_{\rm lab})$: intersection group of *G* and $N_E(U_{\rm lab})$].

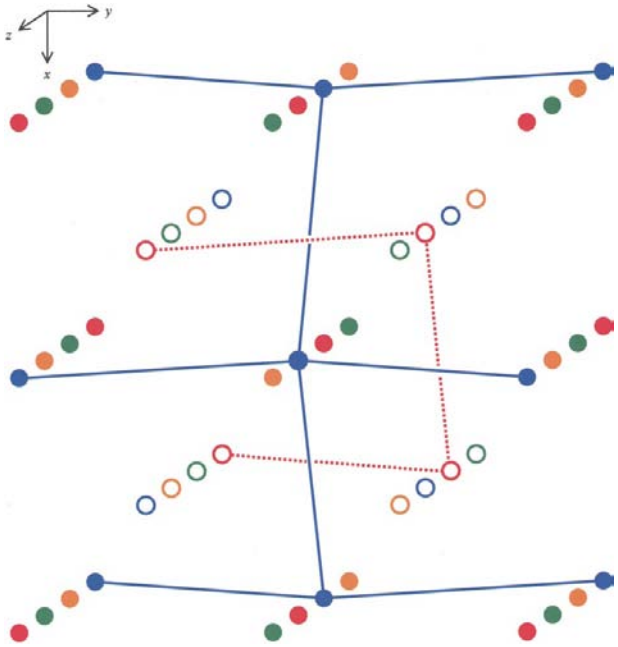

Figure 9
Vertices of the eight labyrinth graphs of an NO3^8–t1 surface. Edges are shown only for two labyrinth graphs.

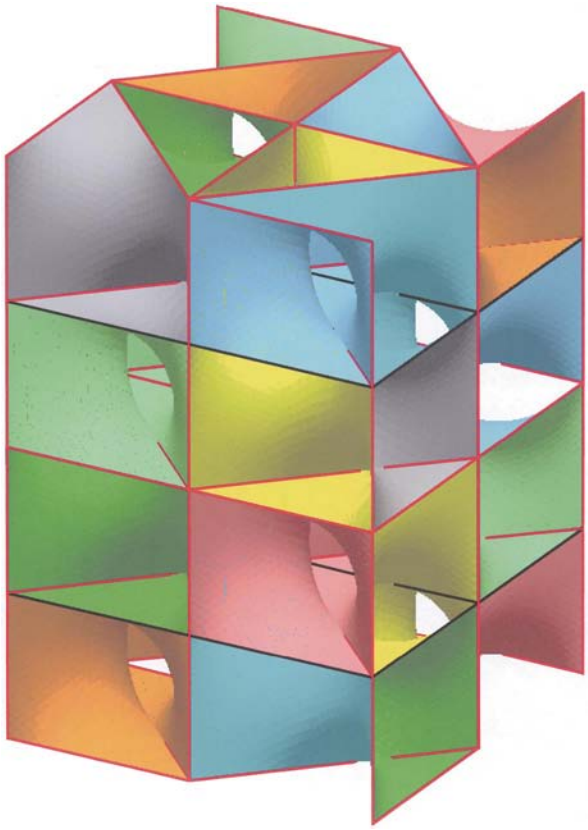

Figure 10
Part of an NO3^8–t2 surface with symmetry $G = I422$. Half of a unit cell of $U_{lab} = I4_122$ (2**a**, 2**b**, 2**c**) is shown. Polygon edges with self-intersections are marked in red.

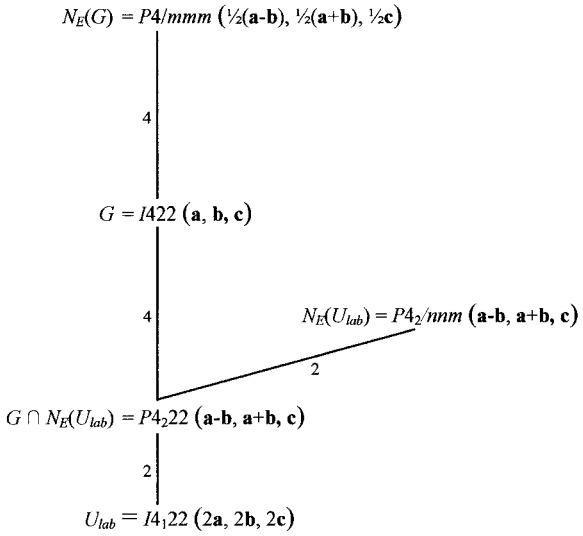

Figure 11
Subgroup diagram referring to an NO3^8–t2 surface [G: symmetry group of the minimal surface; $N_E(G)$: Euclidean normalizer of G; U_{lab}: symmetry group of a labyrinth; $N_E(U_{lab})$: Euclidean normalizer of U_{lab}; $G \cap N_E(U_{lab})$: intersection group of G and $N_E(U_{lab})$].

any crystallographic point group in R^3 but it is the p-Sylow group ($p = 2$) in A_8, where A_8 is the alternating group of degree 8, *i.e.* the group of all even permutations of eight elements (*cf. e.g.* Hall & Senior, 1964).

An NO3^8–t2 surface with symmetry $I422$ also gives rise to eight congruent labyrinths (*cf.* Fig. 10). Each corresponding labyrinth group U_{lab} belongs to type $I4_122$ with $\mathbf{a}' = 2\mathbf{a}$, $\mathbf{b}' = 2\mathbf{b}$

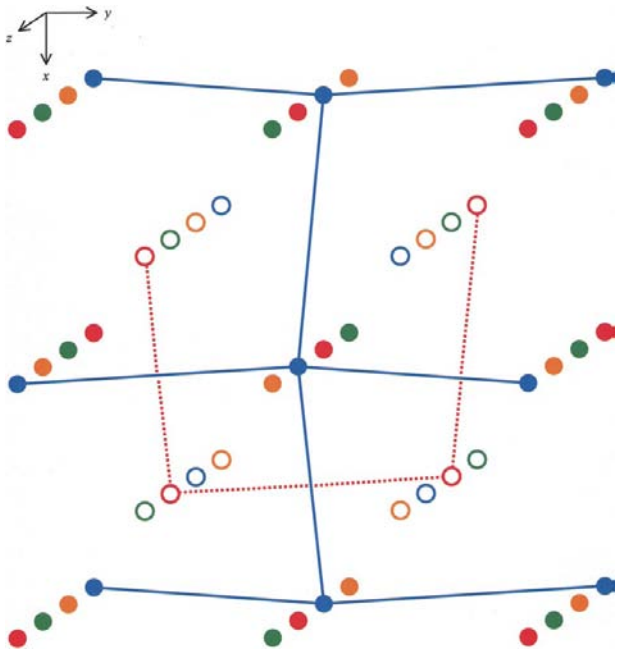

Figure 12
Vertices of the eight labyrinth graphs of an NO3^8–t2 surface. Edges are shown only for two labyrinth graphs.

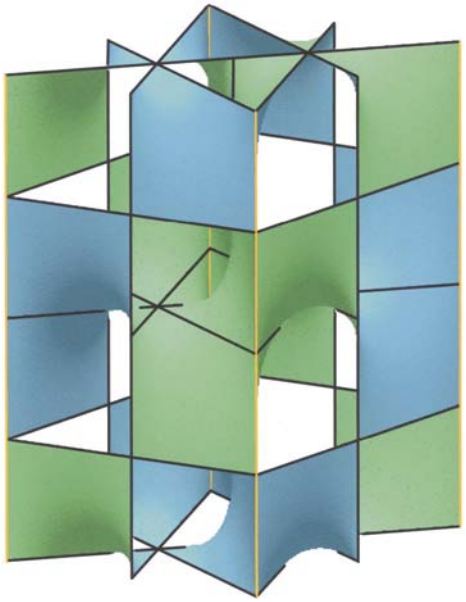

Figure 13
Part of an OR3^2–h2 surface with symmetry $G = P622$. One unit cell of $U_{lab} = P6_322$ (2**c**) is shown. Polygon edges with threefold self-intersections are marked in yellow.

Table 3
Orientable minimal surfaces.

Minimal surface						Labyrinths		
Symbol	Space-group pair G–S	Site symmetry	Generating polygon	χ	b	Symmetry U_{lab}	n_{lab}	χ_{lab}
$OR3^2$–h1	$P6/mcc - P\bar{6}2c$	m..	6-gon	−8	–	$P\bar{6}2c$	2	−8
$OR3^2$–h2	$P622 - P6_322$ (2**c**)		5-gon	−8	–	$P6_322$ (2**c**)	2	−8
$OR3^2$–t1	$P4_222 - P4_322$ (2**c**)		6-gon	−8	–	$P4_322$ (2**c**)	2	−8

and $\mathbf{c}' = 2\mathbf{c}$ and has index 8. The relations between the groups G, U_{lab}, $N_E(G)$, $N_E(U_{lab})$ and $G \cap N_E(U_{lab})$ of an $NO3^8$–t2 surface (*cf.* Fig. 11) are quite analogous to those for an $NO3^8$–t1 surface (*cf.* Fig. 8). Accordingly, each space group of type $I422$ has 16 Euclidean-equivalent subgroups of type $I4_122$ with $\mathbf{a}' = 2\mathbf{a}$, $\mathbf{b}' = 2\mathbf{b}$ and $\mathbf{c}' = 2\mathbf{c}$, four times four of which are conjugate in $I422$, *i.e.* each space group of type $I422$ corresponds to four congruent $NO3^8$–t2 surfaces which differ in their labyrinth groups. Two of the eight labyrinths of each surface have the same labyrinth group and are shifted against each other by a vector **c**. A second labyrinth group of a surface may be derived from a given first one with the aid of a translation by a vector **a**, *i.e.* the 4_1 and 4_3 axes of the two labyrinth groups interchange their positions. The other two labyrinth groups have their 2.. axes at the positions of the 4_1 and 4_3 axes of the first ones.

Again, each labyrinth is adjacent to four other labyrinths belonging to two different labyrinth groups. The 2.. axes of the original labyrinth coincide with the 4_1 and 4_3 axes of its four neighbouring labyrinths.

Considered together, the vertices of the eight labyrinth graphs of an $NO3^8$–t2 surface [$I422$ 4(*d*) $0, \frac{1}{2}, \frac{1}{4}$] also form a C_c configuration, but it is shifted by the vector $(0, \frac{1}{2}, \frac{1}{4})$ against the origin of $I422$. The vertex at $0, \frac{1}{2}, \frac{1}{4}$ is connected to $0, \frac{3}{2}, -\frac{1}{4}$, to $0, -\frac{3}{2}, -\frac{1}{4}$, to $1, 0, \frac{3}{4}$ and to $-1, 0, \frac{3}{4}$. Again, the vertices of each single labyrinth graph form a tetragonal D configuration, but the relative positions of the eight D configurations of an $NO3^8$–t2 surface differ from those referring to an $NO3^8$–t1 surface (*cf.* Fig. 12).

The following pairs of symmetry operations and permutations of eight elements (colours) generate the eight-colour space group corresponding to $I422$–$I4_122$ (2**a**, 2**b**, 2**c**):

$$
\begin{aligned}
&t \quad (1, 0, 0) \quad (14)(23)(58)(67),\\
&t \quad (0, 1, 0) \quad (13)(24)(57)(68),\\
&t \quad (0, 0, 1) \quad (12)(34)(56)(78),\\
&t \quad (\tfrac{1}{2}, \tfrac{1}{2}, \tfrac{1}{2}) \quad (16)(25)(38)(47),\\
&2 \quad 0, 0, z \quad (13)(24)(58)(67),\\
&4^+ \quad 0, 0, z \quad (1835)(2746),\\
&2 \quad 0, y, 0 \quad (14)(23)(56)(78).
\end{aligned}
$$

Although these permutations differ from those for an $NO3^8$–t1 surface, the same permutation group with order 64 is generated.

Table 4
Generating polygons of orientable minimal surfaces.

Symbol	Generating polygon	Previous symbol
$OR3^2$–h1	$00\frac{1}{4} \mid 2/3\,1/3\,\frac{1}{4} \mid \frac{1}{2}0\frac{1}{4} \mid \frac{1}{2}0\frac{3}{4} \mid 2/3\,1/3\,\frac{3}{4} \mid 00\frac{3}{4} \mid 3 \mid$	HAT1–3^2
$OR3^2$–h2	$000 \mid 2/3\,1/3\,0 \mid \frac{1}{2}00 \mid \frac{1}{2}0\frac{1}{2} \mid 00\frac{1}{2} \mid 3 \mid$	HAT2–3^2
$OR3^2$–t1	$000 \mid \frac{1}{2}00 \mid \frac{1}{2}0\frac{1}{2} \mid \frac{1}{2}\frac{1}{2}\frac{1}{2} \mid \frac{1}{2}\frac{1}{2}\frac{3}{4} \mid 00\frac{3}{4} \mid 3 \mid$	

3. Orientable minimal surfaces

Only three families of self-intersecting orientable minimal surfaces which subdivide R^3 into two labyrinths are known so far. They are listed in Tables 3 and 4, which are similar to Tables 1 and 2. The symmetry of such an orientable surface is described by a group–subgroup pair G–S with index 2 in the second column of Table 3. Again, G means the full symmetry of the surface whereas S describes the symmetry of the oriented surface. The site symmetry (if necessary) of a surface patch is displayed in column 3. The Euler characteristic χ is referred to a primitive unit cell of S, as usual for orientable surfaces.

In all three cases, the symmetry group U_{lab} of the two labyrinths and the symmetry group S of the oriented surface are identical. A necessary and sufficient condition for this identity is the following: Along all lines of self-intersection, three parts of the minimal surface intersect and each line of self-intersection corresponds (at least topologically) to a sixfold rotation axis of G and to a threefold rotation axis of S. The only minimal surfaces known so far showing exclusively threefold self-intersections are those listed in Tables 3 and 4. As a consequence of the equivalence of S and U_{lab}, $\chi = \chi_{lab}$ holds in all three cases. As an example, part of an $OR3^2$–h2 surface is shown in Fig. 13.

No self-intersecting orientable minimal surfaces with $S \neq U_{lab}$, which subdivide R^3 into infinite three-periodic labyrinths, are known so far. It is an open question whether or not such surfaces can exist in principle. All known orientable minimal surfaces with $S \neq U_{lab}$ subdivide R^3 either into finite 'polyhedra' or into one-periodic 'tubes'.

The author wishes to thank Dr H. Sowa (Marburg), who first proposed the generating polygon for the $NO3^8$–t1 surfaces, and Professor Dr W. Fischer (Marburg) for helpful discussions.

References

Brakke, K. (1992). *Exp. Math.* **1**, 141–165.
Fischer, W. & Koch, E. (1996*a*). *Z. Kristallogr.* **211**, 1–3.
Fischer, W. & Koch, E. (1996*b*). *Philos. Trans. R. Soc. London Ser. A*, **354**, 2105–2142.
Hall, M. Jr & Senior, J. K. (1964). *The Groups of Order 2^n ($n \leq 6$).* New York: Macmillan.
International Tables for Crystallography (1987). Vol. A, edited by Th. Hahn. Dordrecht: Kluwer Academic Publishers.
Koch, E. & Fischer, W. (1999). *Acta Cryst.* A**55**, 58–64.
Schoen, A. H. (1970). *Infinite Periodic Minimal Surfaces Without Self-Intersections*, NASA Technical Note D-5541.